ARTICLE

Electronic Supplementary Information (ESI)

Characterization

Real-Time of Spark Plasma Sintering

The real-time current, displace, Vac. P, pressure, temperature, and voltage in spark plasma sintering were recorded and analyzed to ensure suitable conditions for the process.

The SEM images of GNS and Sr/Zn-doped CPP/GNS

The SEM was performed according to the way mentioned in main article to observe the product of spark plasma sintering and GNS.

Hardness Measurement and Impact Strength

To select the fillers with the best performance, the hardness measurement and impact strength of composite material were performed according to the way mentioned in the main article.

Morphology of Sr/Zn-doped CPP/GNS/UHMWPE

The micro-morphology of cross-sections of 15% Sr/Zn-doped CPP/GNS/UHMWPE, 20% Sr/Zn-doped CPP/GNS/UHMWPE, 30% Sr/Zn-doped CPP/GNS/UHMWPE were characterized according to the way mentioned in main article.

The CCK-8 test of Sr/Zn-doped CPP/GNS particles

To select the fillers with the best performance on bio-compatibility, the CCK-8 test of Sr/Zn-doped CPP particles and Sr/Zn-doped CPP/GNS particles was performed according to the way mentioned in the main article.

The ELISA test of particles

To prove the aseptic loosening of Sr/Zn-doped CPP/GNS particles, the ELISA test was performed according to the way mentioned in the thesis.

Analysis

Real-Time of Spark Plasma Sintering

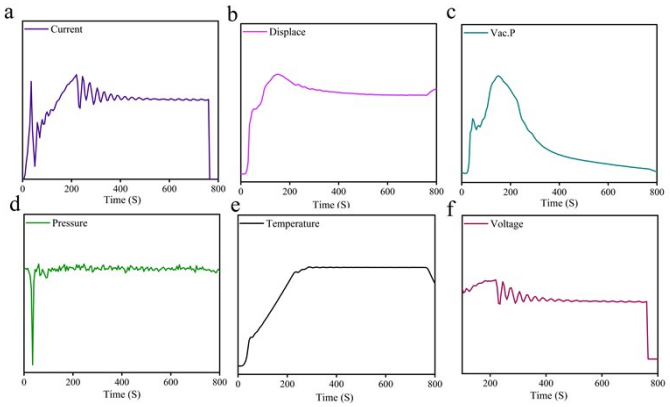

Fig.S1 The Real-Time Data of Spark Plasma Sintering: (a) Current; (b) Displace; (c) Vac.P; (d) Pressure; (e)Temperature; (f) Voltage.

From Fig.1a, we could find that the significant shock current peak, which meant the process of sintering; Fig.1b showed the change of displacing with time, the peak indicated the decrease of inner space led by the crystallization of Sr/Zn-doped CPP/GNS; Fig.1c showed the change of Vac. P with time, which was consistent with the change of displace; Fig.1d showed the change of pressure with time, and the pressure was set at a certain value (40MPa); Fig.1e showed the change of temperature, which corresponded to the process conditions; Fig.1f showed the change of voltage during the process of sintering.

The SEM images of GNS and Sr/Zn-doped CPP/GNS

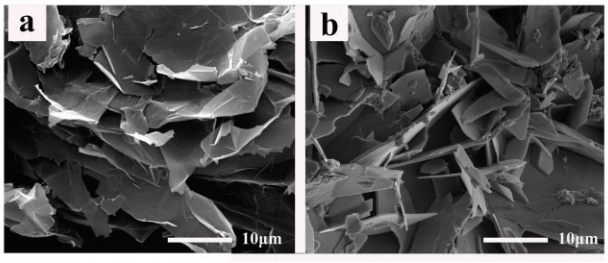

Fig.S2 The SEM images: (a) GNS; (b) Sr/Zn-doped CPP/GNS.

The SEM images of GNS and Sr/Zn-doped CPP/GNS were shown in Fig.S2. From Fig.S2, we could find that the nanosheets are thin while the Sr/Zn-doped CPP/GNS have change to the thick ones due to the combination of GNS and Sr/Zn-doped CPP.

Hardness Measurement and Impact Strength

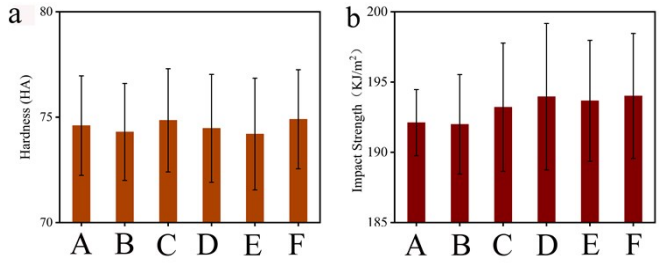

Fig.S3 Hardness, impact strength of 10% Sr/Zn-doped CPP/GNS/UHMWPE composites with various Zn contents: (a) Hardness; (b) Impact Strength. (n=3), 8%Sr/0.00%Zn-doped CPP/UHMWPE (denoted as A); 8%Sr/0.10%Zn-doped CPP/UHMWPE (denoted as B); 8%Sr/0.15%Zn-doped CPP/UHMWPE (denoted as C); 8%Sr/0.20%Zn-doped CPP/UHMWPE (denoted as D); 8%Sr/0.25%Zn-doped CPP/UHMWPE (denoted as E); 8%Sr/0.30%Zn-doped CPP/UHMWPE (denoted as F).

Our previous research had indicated that 10%Sr-doped CPP/UHMWPE exhibited good comprehensive performances. Thus, we used 10% Sr-doped CPP/UHMWPE as a reference to explore the influence of different content of ion on the hardness and impact strength of materials. The results showed that the doping of trace zinc had no significant effect on the hardness and impact strength of the Sr/Zn-doped CPP/UHMWPE composite materials.

Morphology observation of Sr/Zn-doped CPP/GNS/UHMWPE

Fig.S4 The SEM images: (a) The cross-section of 15% Sr/Zn-doped CPP/GNS/UHMWPE; (b) The cross-section of 20% Sr/Zn-doped CPP/GNS/UHMWPE; (c) The cross-section of 30% Sr/Zn-doped CPP/GNS/UHMWPE.

The excessive addition of Sr/Zn-doped CPP/GNS resulted in the existence of voids and agglomerates, which reduced the ability of composite materials to absorb stress and impact energy by forming weak points of stress concentration around the enhanced-particles. Besides, the poor adhesion of fillers to the matrix materials caused by large agglomerates resulted in the fall-off of fillers from the matrix under impact force, which significantly reduced the impact strength of composite material.

The CCK-8 test of various Sr/Zn-doped CPP and Sr/Zn-doped CPP/GNS particles

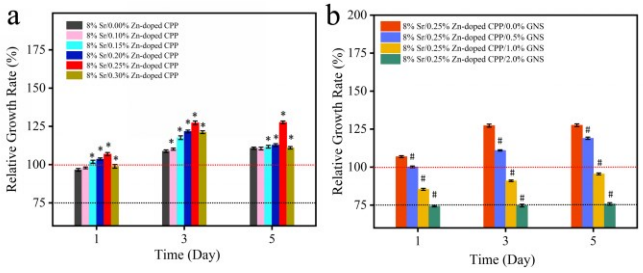

Fig.S5 The CCK-8 Test of various particles:(a) Sr/Zn-doped CPP;(b) Sr/Zn-doped CPP/GNS(n=3, * means the difference attained a statistically significant difference compared to the 8%Sr/0.00%Zn-doped CPP group, $p<0.05$; # means the difference attained a statistically significant difference compared to the 8%Sr/0.25%Zn-doped CPP/0.0% GNS group, $p<0.05$).

Wear particles could perform stimulation effects on the proliferation of cells, which then changed the expression of molecular factors. Therefore, we researched the effects of wear particles on MC3T3-E1at at different times. Fig.2 showed the result about the proliferation of MC3T3-E1 challenged by various wear Sr/Zn-doped CPP particles. The cells challenged by8% Sr-doped CPP particles were set as the control. The relative growth rate (RGR) showed that cell proliferation increased with the increase of culture time. In short, the proliferation rate ofMC3T3-E1 cells challenged by various Sr/Zn-doped CPP particles increased in a Zn content-dependent way. From Fig.2a, we could find that the 8%Sr/0.25%Zn-doped CPP showed the highest RGR, which meant its best promotion effects on the proliferation of MC3T3-E1. In general, suitable-dose addition of Zn increased the proliferation of osteoblasts. The reason might be that the co-doping of Sr and Zn enhanced the biological properties of particles on the adhesion and proliferation of osteoblasts through the signal transduction pathway of osteogenic differentiation[1-4].

At the same time, we explored the effects of graphene nanosheets (GNS) on the proliferation of MC3T3-E1according to the method above. The analysis was shown in Fig.2b. The cells challenged by 8%Sr/0.25%Zn-doped CPP particles were chosen as the control. RGR values showed that the cell proliferation increased with the increase of culture time, but decreased with the increase of GNS content added, which meant that the addition of GNS inhibited the proliferation of MC3T3-E1. The molecular mechanisms underlying this was that the GNS disrupted the structure and function of the protein by particularly strong inter-molecular interactions[5]. Previous studies indicated that GNS can affect the structure of the peptide[6], which inhibited the proliferation of MC3T3-E1. Finally，we used the 8%Sr/0.25%Zn-doped CPP/0.5%GNS particles as fillers to enhance UHMWPE.

The ELISA test of Sr/Zn-doped CPP/GNS particles

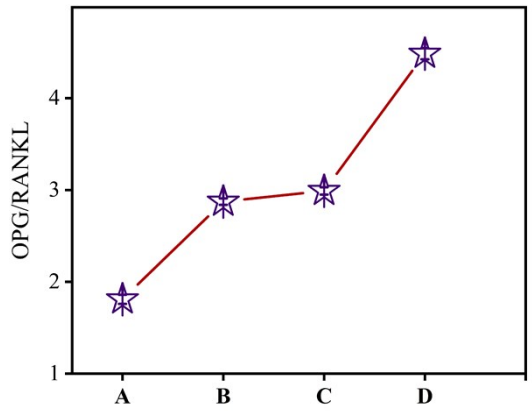

Fig.S6 The effect of particles on OPG/RANKL ratio from MC3T3-E1 at 48 h (n=3): CPP/0.25%GNS(denoted as A); 8%Sr-doped CPP/0.25%GNS (denoted as B); 0.25%Zn-doped CPP/0.25%GNS (denoted as C); 8%Sr/0.25% Zn-doped CPP/0.5% GNS(denoted as D).

Sr/Zn-doped CPP/GNS could increase the OPG/RANKL ratio by promoting the production of OPG from osteoblasts and inhibited the production of RANKL by osteoblasts. The OPG/RANKL ratio presented from MC3T3-E1 challenged by Sr/Zn-doped CPP/GNS was significantly higher than that of cells challenged by Sr-doped CPP. This might be due to that the Sr/Zn-doped CPP/GNS exerted their stronger therapeutic effect by down-regulating sclerostin, thereby activating the Wnt/beta-catenin signal pathway[7].

Table.1: The abbreviations.

Abbreviations	Explanation
CPP	Calcium Polyphosphate
GNS	Graphene Nanosheets
Sr/Zn-doped CPP	Sr, Zn co-doped CPP
Sr/Zn-doped CPP+GNS	the solid mixing product of amorphous Sr/Zn-doped CPP powders and GNS
Sr/Zn-doped CPP/GNS	the spark plasma sintering product of Sr/Zn-doped CPP powders and GNS
UHMWPE	Ultra-High Molecular Weight Polyethylene
Sr/Zn-doped CPP/GNS/UHMWPE	the hot press product of Sr/Zn-doped CPP/GNS and UHMWPE
Sr-Zn-doped CPP/UHMWPE	the hot press product of Sr/Zn-doped CPP and UHMWPE
COF	Coefficient of Friction
MC3T3-E1	Mouse Embryo Osteoblast Precursor Cells
MEM	Minimum Essential Medium
P3	Passage 3
CCK-8	Cell Counting Kit-8
OPG	Osteoprotegerin
RANKL	Receptor Activator of Nuclear Factor-κ B Ligand
ELISA	Enzyme Linked Immunosorbent Assay

Reference

1. I. Ullah, M. A. Siddiqui, S. K. Kolawole, H. Liu, J. Zhang, L. Ren and K. Yang, *Ceram. Int.*, 2020, **46**, 14448-14459.
2. B. Jia, H. Yang, Z. Zhang, X. Qu, X. Jia, Q. Wu, Y. Han, Y. Zheng and K. Dai, *Bioactive materials*, 2021, **6**, 1588-1604.
3. Z. Dai, M. Wang, S. Wang, J. Li, X. Chen, D.-L. Wang and Y.-C. Zhu, *Journal of Inorganic Materials*, 2020, **35**, 179-186.
4. S. Murphy, A. W. Wren, M. R. Towler and D. Boyd, *J. Mater. Sci.-Mater. Med.*, 2010, **21**, 2827-2834.
5. L. Ou, Y. Luo and G. Wei, *J Phys Chem B*, 2011, **115**, 9813-9822.
6. N. Cobelli, B. Scharf, G. M. Crisi, J. Hardin and L. Santambrogio, *Nature Reviews Rheumatology*, 2011, **7**, 600-608.
7. B. Wang, H. Guo, T. Geng, K. Sun, L. Zhang, Z. Lu and Q. Jin, *Bioscience reports*, 2021, DOI: 10.1042/bsr20203003.